Precision Measurements of Nucleon and Nuclear Structure Functions to Constrain Gluon Distributions

P. E. C. Markowitz

Florida International University, Miami FL, 33199, USA

A. Accardi, I. Albaryrak, O. Ates, A. Bruell, C. Chen, M. E. Christy(spokesperson), C. Jackson, C. E. Keppel(spokesperson), M. Kohl, Y. Li, P. Monaghan, A. Pushpakumari, L. Tang, J. Taylor, T. Walton, Z. Ye, L. Yuan, and L. Y. Zhu(spokesperson)

Hampton University, Hampton, VA 23668, USA

B. T. Hu

Lanzhou University, Lanzhou, Gansu Province, China

X. Jiang and A. Puckett

Los Alamos National Laboratory, Los Alamos, NM 87544, USA

V. Sulkosky

Massachusetts Institute of Technology, Cambridge, MA 02139, USA

D. Dutta

Mississippi State University, Mississippi State, MS 39762, USA

R. Ent, D. Gaskell, V. Guzey, M. Jones, and P. Solvignon

Thomas Jefferson National Accelerator Facility, Newport News, VA 23606, USA

S. P. Malace

University of South Carolina, Columbia, SC 29206, USA

G. Huber

Univ. of Regina, Regina, SK S4S0A2, Canada.

H. Baghdasaryan, D. Day, N. Kalantarians, and V. Mamyan

University of Virginia, Charlottesville, VA 22904, USA

A. Asaturyan, A. Mkrtchyan, H. Mkrtchyan, V. Tadevosyan, and S. Zhamkochyan

Yerevan Physics Institute, 2 Alikhanyan Brothers St., Yerevan 0036, Armenia

(Dated: December 14, 2009)

Abstract

We propose to measure inclusive cross sections on a range of nuclei, including: H, D, C, Al, Ca, Sn, in the range $0.2 < Q^2 < 3.8$ (GeV/c)^2. The data will provide significant checks to verify (or not) the positive slope in the logarithmic derivative of the $F_2^{Sn}/F_2^C(Q^2)$ from the NMC data, which has a significant impact on nuclear modifications to the gluons extracted from nuclear parton distribution fits. Additionally we will perform separations of the longitudinal and transverse cross sections to aid in unambiguously separating F_L from F_2. The longitudinal structure function F_L has long been advocated as a direct probe of the gluon density. Specifically, the new data will facilitate the study of the transition of F_L (and hence $R = \sigma_L/\sigma_T$) to the nonperturbative regime, where previous JLab data hint that there might already be a difference in R (F_L) between proton and deuteron. This will be accomplished by adding additional dedicated precision L/T separations in the DIS region and by adding additional cross section measurements in the resonance region at higher ϵ than what was obtainable with a 6 GeV beam. This new resonance region data, in combination with existing data Hall C data, will reduce the current F_L uncertainties by a factor of 2 or more in this region. The impact of the entire proposed data will reduce the uncertainties by a factor of 2 for the n=4 F_L moments and by an even larger factor for the higher moments.

Contents

1. INTRODUCTION

Since the early lepton scattering experiments discovered the substructure of the nucleon and led to the development of the quark-parton model, deep inelastic scattering (DIS) has proved to be a critical tool in the investigation of nucleon and nuclear structure. While the F_2 structure function is sensitive to the nucleon gluon distribution only through it's logarithmic Q^2 dependence in pQCD, the longitudinal structure function F_L is directly sensitive to the glue. A set of closely linked measurements are proposed to study both F_L^A and the Q^2 dependence of F_2 in nuclei. Such measurements will directly benefit both nuclear parton distribution (nPDF) studies and testing of theoretical models of nuclear modifications to structure functions. In addition, we propose measurements which will significantly improve the determination of the nucleon F_L moments around $Q^2 \sim 4$ (GeV/c)^2.

The proposed measurements are all inclusive scattering, which would be performed utilizing the standard equipment in Hall C after the 12 GeV upgrade, and exploiting the expertise of the collaborators in performing precision cross section measurements. Such measurements naturally fit into an integrated run period which would utilize a common set of nuclear targets, beam, and base equipment. The three closely related physics topics to be studied are listed below, and will be discussed in detail in the noted sections.

- [**Nuclear F_2 ratio at $x < 0.1$**] **(Section 3.1)**

  First, we propose to investigate evidence for a nontrivial Q^2 dependence in the F_2 structure function ratio for different nuclei at $0.01 < x < 0.1$. This Q^2 dependence provides sensitivity to the nuclear gluon distribution determined in nPDF fits. If nuclear modifications such as shadowing were the same in both F_2 and the gluons then a flat Q^2 dependence would be expected. However, the precise Sn/C F_2 data from the NMC collaboration indicated a clear positive slope with $\ln(Q^2)$, which indicated a nontrivial nuclear dependence of the gluon distributions. However, this nontrivial Q^2 dependence was not seen in other nuclear ratios, like C/D and Ca/D data from NMC. We propose to provide data which will for the first time provide a direct check of the NMC results and will help to finally resolve this long standing puzzle.

- [**Nuclear dependence of F_L and $R = \sigma_L/\sigma_T$ for $0.4 < Q^2 < 3$**] **(Sections 3.2)**

  Second, we propose to measure ratios of F_L and R for different nuclear targets (H, D, C, Al, Ca, Sn), in the range $0.4 < Q^2 < 3.3$ (GeV/c)^2. A nontrivial Q^2 dependence in F_2^{Sn}/F_2^C due to differences in the nuclear modifications between F_2 and the glue *must* be reflected in a nonzero value for $R^{Sn} - R^C$ at small x and Q^2 at which pQCD is expected to hold, and we propose to provide just such a check. In addition, we will propose to measure at smaller Q^2 to study the approach of the structure functions to the real photon limit. This will help us to have a better understanding of the nuclear modifications to the structure functions in the non-perturbative region. There is a hint from JLab experiment E99-118 that R for deuterium is smaller than that for hydrogen. If this is due to the nuclear effects, the deviation is expected to be bigger in heavier nuclei.

- [F_L **moments at $Q^2 = 3.75$**] **(Section 3.3)** Third, we propose to make measurements

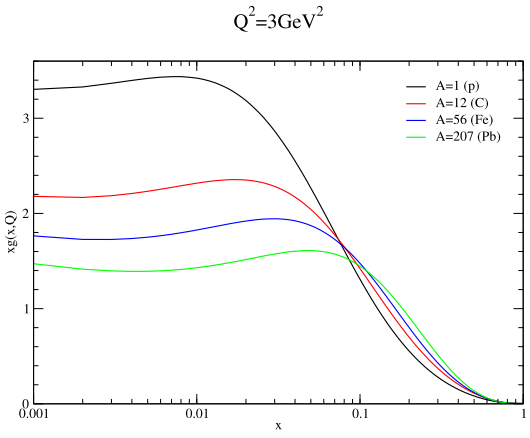

FIG. 1: [1] The gluon distributions as a function of Bjorken x for different nuclei, following the CTEQ formalism.

which will significantly improve determinations of the higher F_L moments around $Q^2 \sim 4$ (GeV/c)^2 in both proton and deuteron targets. In addition to comparing $2F_2^p - F_2^d$ with the Lattice calculation, measuring F_L for both targets provides additional constraints on the separation of the singlet and non-singlet moments. The increased CEBAF beam energy not only allows for new precision measurements at lower x at this Q^2, but will also help to significantly improve the existing Rosenbluth separations from E94-110 (proton) and E06-109 (deuteron) by virtue of additional cross section measurements at higher ϵ values and extending the ϵ coverage of the existing data sets.

2. FORMALISM

Due to the small value of the electromagnetic coupling constant, the scattering of electrons from nucleons can be well approximated by the exchange of a single virtual photon, which carries the exchanged 4-momentum squared, q^2. In terms of the incident electron energy E, the scattered electron energy $E^{'}$, and the scattering angle θ, the absolute value of the exchanged 4-momentum squared is given by

$$Q^2 = -q^2 = 4EE^{'}\sin^2\frac{\theta}{2}. \quad (1)$$

In this one photon exchange approximation, the spin-independent cross section for inclusive electron-nucleon scattering can be expressed in terms of the photon helicity coupling as

$$\frac{d^2\sigma}{d\Omega dE'} = \Gamma \left[\sigma_T(x,Q^2) + \epsilon\sigma_L(x,Q^2)\right], \tag{2}$$

where σ_T (σ_L) is the cross section for photo-absorption of purely transverse (longitudinal) polarized photons, and Bjorken x is the fraction of the momentum carried by the quarks and gluons and can be expressed as $x = \frac{Q^2}{2M(E-E')}$ in the lab frame with target mass M.

$$\Gamma = \frac{\alpha E^{'}(W^2 - M^2)}{4\pi^2 Q^2 M E(1-\epsilon)} \tag{3}$$

is the flux of transverse virtual photons with strong coupling constant α, invariant mass W and $\nu = E - E^{'}$, and the virtual photon polarization parameter

$$\epsilon = \left[1 + 2(1 + \frac{\nu^2}{Q^2})\tan^2\frac{\theta}{2}\right]^{-1} \tag{4}$$

with $\epsilon = 0$ for purely transverse polarization. It can be also expressed in terms of $y = \nu/E$ and Q^2/E^2

$$\epsilon = \frac{4(1-y) - \frac{Q^2}{E^2}}{4(1-y) + 2y^2 + \frac{Q^2}{E^2}}\ . \tag{5}$$

At small Q^2 ($<< E^2$), ϵ only depends on y, with the relation $\epsilon = 1 - \frac{y^2}{1+(1-y)^2}$. This implies that $\epsilon = 1$ at $y = 0$, and $\epsilon = 0$ at $y = 1$. The study of the ϵ dependence at JLab and HERMES, is equivalent to the study of the $\frac{y^2}{1+(1-y)^2}$ dependence at H1 and ZEUS at small Q^2.

In terms of the structure functions $F_1(x,Q^2)$ and $F_2(x,Q^2)$ in the DIS scattering, the double differential cross section can be written as

$$\frac{d^2\sigma}{d\Omega dE'} = \Gamma\frac{4\pi^2\alpha}{x(W^2-M^2)}\left[2xF_1(x,Q^2) + \epsilon\left((1+\frac{4M^2x^2}{Q^2})F_2(x,Q^2) - 2xF_1(x,Q^2)\right)\right]. \tag{6}$$

The comparison of Equation 2 and 6 shows that $F_1(x,Q^2)$ is purely transverse, while the combination

$$F_L(x,Q^2) = (1+\frac{4M^2x^2}{Q^2})F_2(x,Q^2) - 2xF_1(x,Q^2) \tag{7}$$

is purely longitudinal. The separation of the unpolarized structure functions into longitudinal and transverse parts from cross section measurements can be accomplished via the Rosenbluth technique [2], by making measurements at two or more ϵ points at fixed x

and Q^2. Fitting the reduced cross section, $d\sigma/\Gamma$, linearly in ϵ, yields σ_T (and therefore $2xF_1(x,Q^2)$) as the intercept, and σ_L (and therefore $F_L(x,Q^2)$) as the slope. Then the longitudinal to transverse cross section ratio $R(x,Q^2) = \sigma_L/\sigma_T = F_L(x,Q^2)/2xF_1(x,Q^2)$ can be easily obtained.

At $Q^2 \to 0$, the virtual photon will approach the real photon limit, where there is no longitudinal components and $R = 0$. Therefore one expects $R \to 0$ at the limit of $Q^2 \to 0$. This can be also derived from the general definition of the hadronic tensor:

$$W^{\mu\nu} = \frac{F_1}{M}\left(-g^{\mu\nu} + \frac{q^\mu q^\nu}{q^2}\right) + \frac{F_2}{M(p\cdot q)}\left(p^\mu - \frac{p\cdot q}{q^2}q^\mu\right)\left(p^\nu - \frac{p\cdot q}{q^2}q^\nu\right) \tag{8}$$

and it can be rearranged in the form

$$W^{\mu\nu} = -\frac{F_1}{M}g^{\mu\nu} + \frac{F_2}{M(p\cdot q)}p^\mu p^\nu + \left(\frac{F_1}{M} + \frac{F_2}{M}\frac{p\cdot q}{q^2}\right)\frac{q^\mu q^\nu}{q^2} - \frac{F_2}{M}\frac{p^\mu q^\nu + q^\mu p^\nu}{q^2} \tag{9}$$

To eliminate the potential kinematic singularities of $W^{\mu\nu}$ at $Q^2 \to 0$ requires that $F_2 = O(Q^2)$ and $\frac{F_1}{M} + \frac{F_2}{M}\frac{p\cdot q}{q^2} = O(Q^2)$. Therefore $F_L = (1+\frac{Q^2}{\nu^2})F_2 - 2xF_1 = O(Q^4)$ and $R = \frac{F_L}{2xF_1} = O(Q^2)$ vanishes when $Q^2 \to 0$ at fixed ν.

Several high precision experiments have utilized the Rosenbluth technique to form a successful 6 GeV program of inclusive, longitudinal/transverse (L/T) separated, precision structure functions measurements in Hall C at Jefferson Lab [3–8]. This program has significantly expanded the global data of structure function measurements on the nucleon and nuclei, and has been used to study various physics topics, such as quark-hadron duality and moment analysis.

With Rosenbluth technique studying the ϵ/y-dependence, the longitudinal structure function F_L can be directly determined. Based on recent H1 data [10], F_L is averaged to be around 0.25, which is also consistent with the dipole models. However, a model dependent extraction from H1 F_2 alone suggests R is around 0.5, which is twice higher than that from the direct measurement of F_L with Rosenbluth technique.

The upcoming 11 GeV beam will expand kinematics that can be achieved at 5.7 GeV beam, as shown in Figure 2. In particular, we propose to focus the kinematics at low x and Q^2, which is sensitive to the gluon contributions.

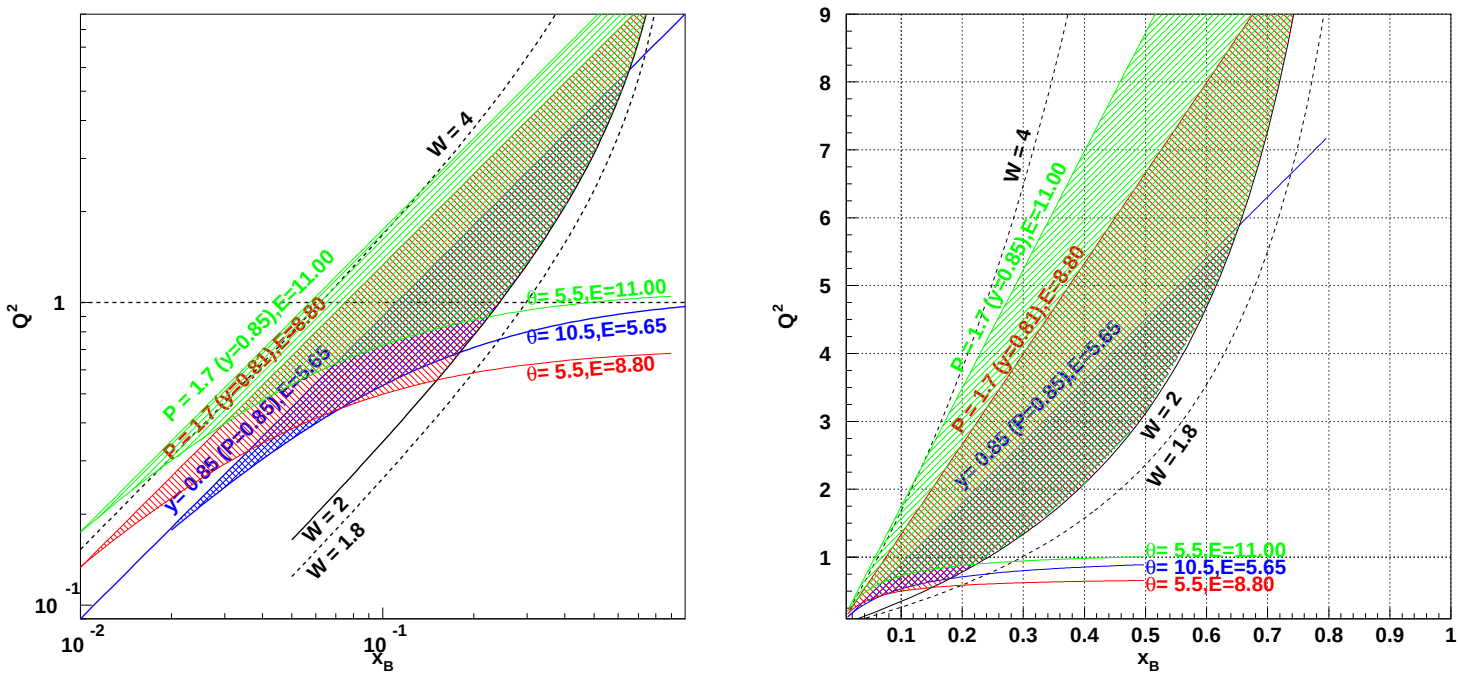

FIG. 2: The kinematics at different beam energies with HMS ($E_e = 5.65$ GeV) or SHMS ($E_e = 8.8, 11.0$ GeV) spectrometer. The kinematics is plotted in logarithmic (left panel) and linear (right panel) scale.

3. PHYSICS MOTIVATION AND PROPOSED MEASUREMENTS

3.1. Q^2 Dependence of F_2^A/F_2^D at $x < 0.1$

Over the past 20 years several measurements at CERN and Fermilab have firmly established that structure functions in nuclei differ significantly from those in free nucleons. The nucleus can not be simply described as a collection of nucleons on mass hell. The normalized F_2^A deviates from the simple expectation of $(ZF_2^p + (A-Z)F_2^n)/A$ as a function of Bjorken x. For isoscalar target with $Z = A - Z$, the normalized F_2^A deviates from F_2^D. Figure 3 shows as an example the ratio of inclusive deep-inelastic cross sections of iron to that of deuterium as measured by the EMC collaboration [9]. The deviation has a clear dependence on Bjorken x, and it was separated into four regions around where F_2^A/F_2^D crosses the unit line.

While the x dependence of these nuclear ratios is well measured, their Q^2 dependence is

Q^2	x_b	E	E'	θ	ϵ	y	W
0.210	0.0124	11.0	2.0	5.6	0.35	0.82	4.19
0.292	0.0173	11.0	2.0	6.6	0.35	0.82	4.18
0.428	0.025	11.0	2.0	8.0	0.35	0.82	4.16
0.591	0.035	11.0	2.0	9.4	0.35	0.82	4.14
0.765	0.045	11.0	2.0	10.7	0.35	0.82	4.12
0.930	0.055	11.0	2.0	11.8	0.35	0.82	4.10
1.180	0.070	11.0	2.0	13.3	0.35	0.82	4.07
1.519	0.090	11.0	2.0	15.1	0.34	0.82	4.03
2.106	0.125	11.0	2.0	17.8	0.34	0.82	3.96
2.950	0.175	11.0	2.0	21.1	0.34	0.82	3.85
0.305	0.025	8.8	2.2	7.2	0.47	0.75	3.60
0.435	0.035	8.8	2.2	8.6	0.47	0.75	3.58
0.554	0.045	8.8	2.2	9.7	0.47	0.75	3.57
0.686	0.055	8.8	2.2	10.8	0.46	0.75	3.55
0.860	0.070	8.8	2.2	12.1	0.46	0.75	3.51
1.118	0.090	8.8	2.2	13.8	0.46	0.75	3.49
1.556	0.126	8.8	2.2	16.3	0.46	0.75	3.42
2.176	0.176	8.8	2.2	19.3	0.45	0.75	3.33
0.208	0.035	6.6	3.43	5.5	0.85	0.48	2.57
0.233	0.045	6.6	3.84	5.5	0.89	0.42	2.41
0.252	0.055	6.6	4.16	5.5	0.92	0.37	2.28
0.274	0.070	6.6	4.51	5.5	0.95	0.32	2.13
0.295	0.090	6.6	4.85	5.5	0.97	0.26	1.97
0.319	0.125	6.6	5.24	5.5	0.98	0.21	1.76
0.338	0.175	6.6	5.50	5.5	0.99	0.16	1.57

TABLE I: The proposed kinematics to measure the Q^2 dependence of the nuclear F_2 ratio with SHMS (red or black)/HMS (black).

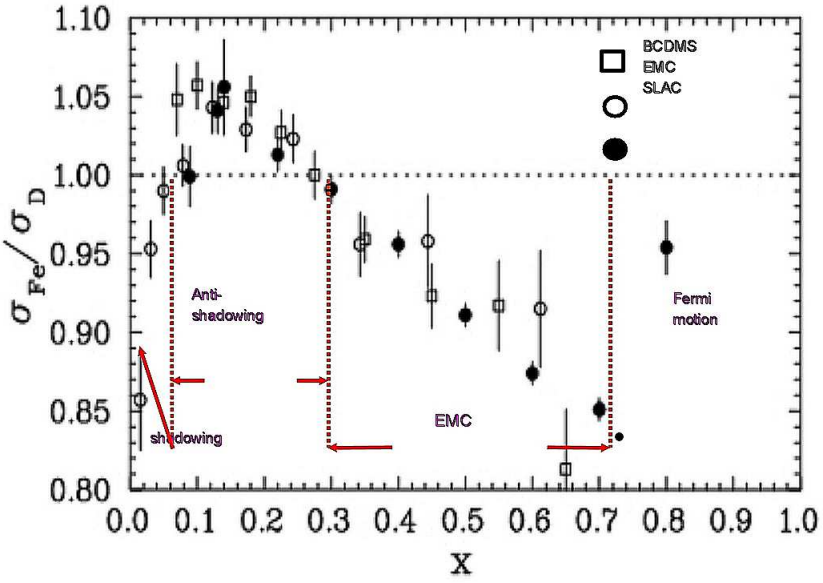

FIG. 3: [9] Iron to deuterium cross section ratio σ_{Fe}/σ_D as a function of x from EMC (hollow circles), SLAC (solid circles) and BCDMS (squares). The data has been averaged over Q^2 and corrected for neutron excess.

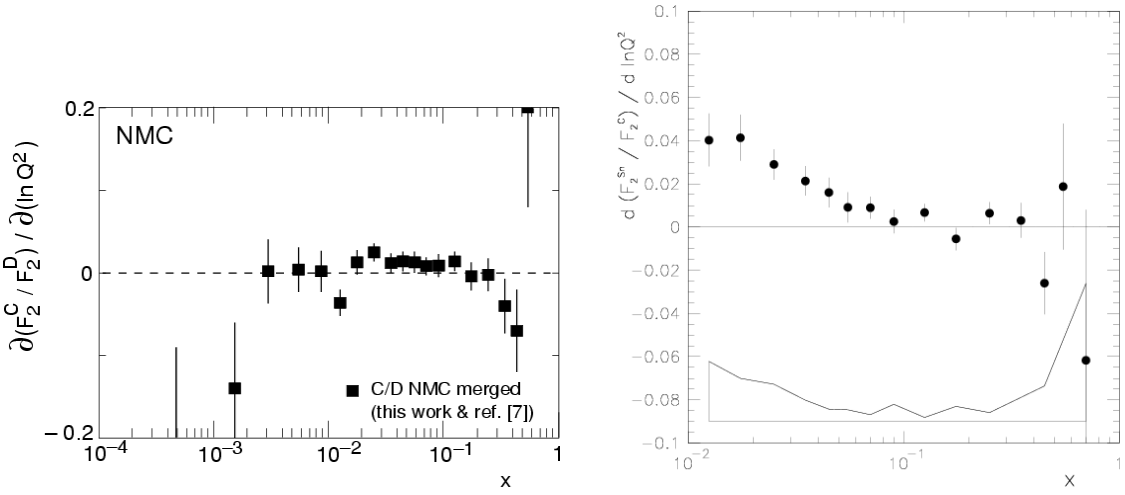

FIG. 4: Logarithmic Q^2 slopes of the structure function ratios carbon and deuterium (left [14]) and tin over carbon (right [15]) as a function of x.

not well studied. Figure 4 shows the two most precise results, both measured by the NMC collaboration but with different experimental setup. On the left is the measurement of C/D which covers a very large range in x and has small systematic uncertainties [14]. On the right is the the measurement of Sn/C with limited x range and significantly larger systematic

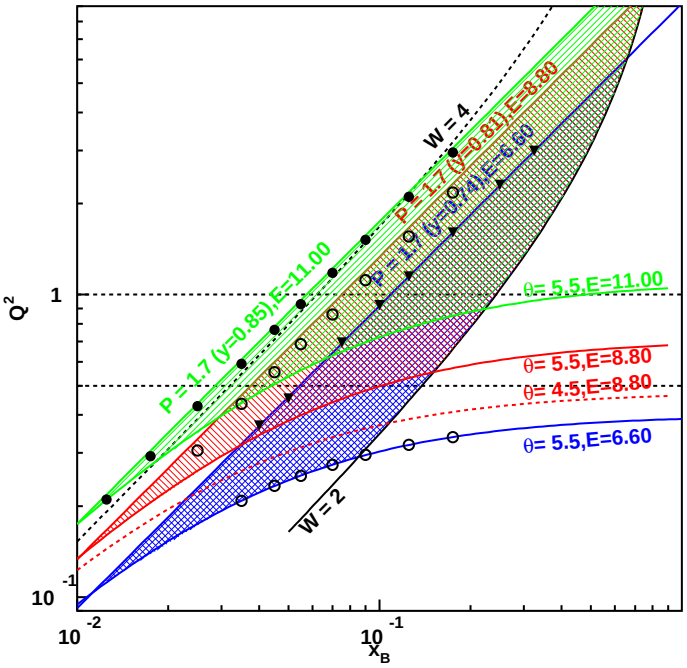

FIG. 5: The proposed kinematics with 11 GeV beam (in solid circles) and 6.6, 8.8 GeV beam (open circles) to study the Q^2 dependence of the F_2^{A1}/F_2^{A2}, i.e. $d(F_2^{A1}/F_2^{A2})/d\ln Q^2$ as a function of Bjorken x. The proposed R measurement were plotted in triangles and will be discussed later.

uncertainties but much higher statistical precision [15]. Obviously, the conclusion from these two measurements are different: while no dependence on Q^2 is observed in the C/D ratio, the Sn/C data show a small but significant positive Q^2 dependence for $0.01 < x < 0.1$. This positive Q^2 dependence has important consequences for nuclear parton distributions and theoretical descriptions of shadowing. It is very sensitive to the nuclear modifications of the gluon distribution. The Q^2 dependence of the NMC Sn/C data can be described by the nuclear parton distribution functions with DGLAP evolutions, at least partially [20]. But it seems to be different with NMC C/D data as well as NMC He/D, Ca/D [13] and the HERMES Kr/D data. This kind of difference makes it difficult to extract precise nuclear gluon distributions within the leading-twist DGLAP approach [20].

With an energy upgraded CEBAF, a significant check on the Q^2 dependence of the NMC Sn/C ratios can be performed with relatively modest beam time. Thus, we propose to measure the ratio σ^A for various nuclei (C, Al, Ca, and Sn) at $0.01 < x < 0.1$. Although

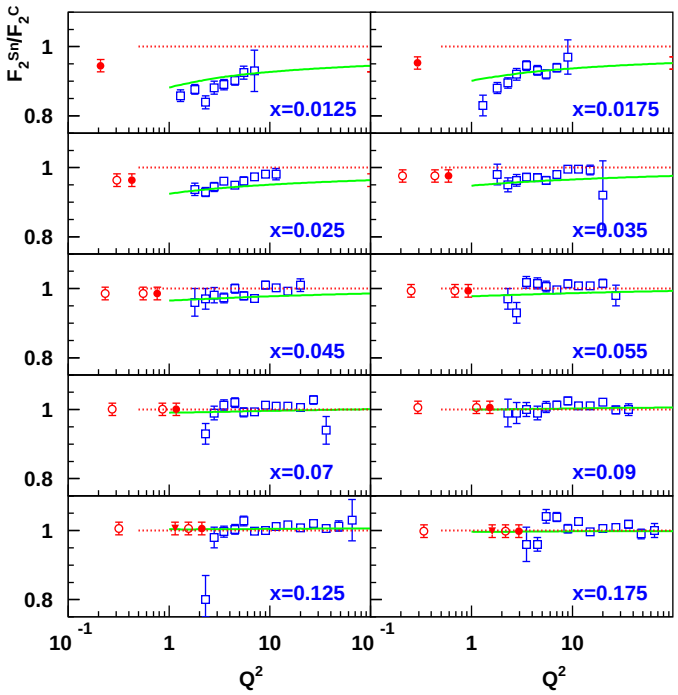

FIG. 6: The projected (F_2^{Sn}/F_2^C) with 11 GeV beam (solid circles) and 6.6/8.8 GeV beam (open circles), and from the R_A measurements (solid triangles), as a function of Bjorken Q^2 for different x bins. The NMC data [15] were plotted in open squares. The 1.8% uncertainty was assumed for the measurements of F_2^{Sn}/F_2^C including 1% relative uncertainty and 1.5% uncertainty in relative normalization. The solid curves are based on the parameterization for NLO nuclear PDFs [20]. The projected data are assumed to have the same (F_2^{Sn}/F_2^C) ratios as were predicted by the nuclear PDFs at $Q^2 = 100$ GeV^2.

these measurements will be performed at smaller values of Q^2 than probed by NMC (see Figure 5), they will clearly allow a determination of whether there is an unknown systematic in that data.

3.2. Nuclear dependence of F_L and R for $0.4 < Q^2 < 3$

For fixed scattering angle, ϵ decreases as the x decreases. For NMC kinematics [14] as an example, $\epsilon < 0.68$ when $x < 3.5 \times 10^{-3}$. When ϵ is small, one must also determine R in order to extract F_2 from cross section measurements. Therefore, we plan to perform Rosenbluth separations to extract R_A for a range of kinematics. In addition to allowing a

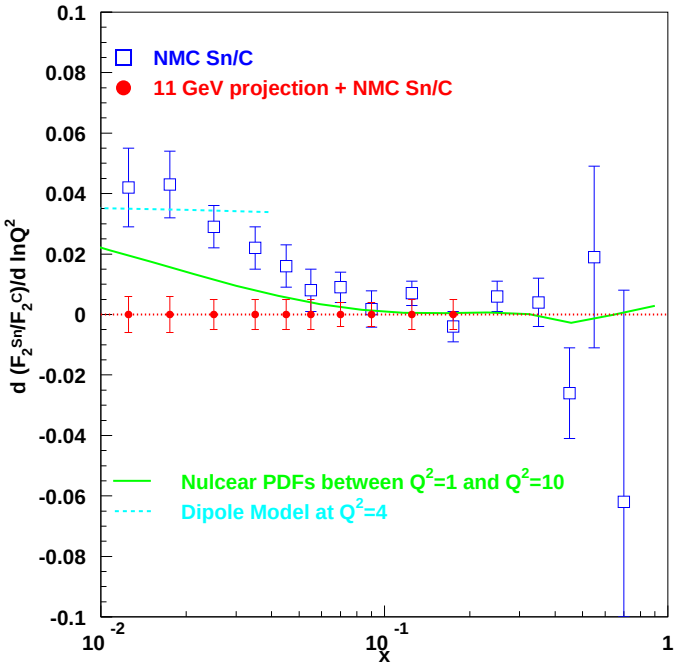

FIG. 7: The projected $d(F_2^{Sn}/F_2^C)/d\ln Q^2$ as a function of Bjorken x (red solid circles), with uncertainties from a combined linear fit of the projected 11 GeV data and NMC data. The NMC data were also plotted. The solid curves are based on the parameterization for NLO nuclear PDFs [20]. The dashed curves are based on a Dipole Model [22].

more accurate determination of F_2^A, R_A itself is sensitive to the nuclear gluon distribution in the perturbative regime and its nuclear dependence should be manifest in R_A as well.

The nuclear effects on $R = \sigma_L/\sigma_T$ in DIS were measured by HERMES collaboration [21] via fitting the cross section ratio σ_A/σ_D as a function of virtual photon polarization ϵ over a typical range of $0.4 < \epsilon < 0.7$. Overall no significant ϵ-dependence was observed for $\sigma_{^{14}N}/\sigma_D$ and $\sigma_{^3He}/\sigma_D$. However at low x ($0.01 < x < 0.03$), R_A/R_D seems to be greater than 1. Since the ϵ-dependence at HERMES may be coupled with Q^2-dependence due to a single beam energy, it is very essential to improve the precision of the HERMES measurement in the low x region with real Rosenbluth techniques. Sizable nuclear modification was observed in $R_D - R_P$ from JLab E99-118 experiment, as shown in Figure 8 [4]. The preliminary data from JLab E00-002 experiment also indicated negative Rd-Rp in this kinematic range [5]. As nuclear modification is expected to be bigger with heavier targets, it is important to

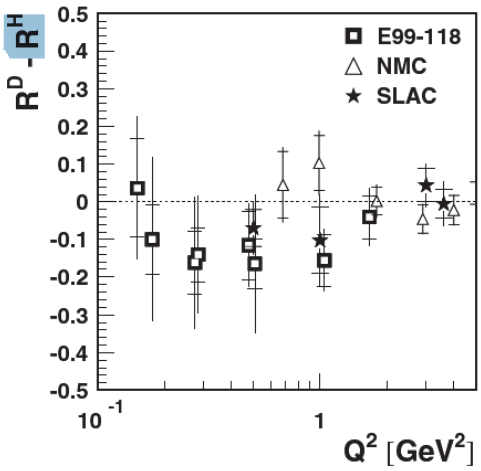

FIG. 8: [4] The difference between R_D and R_P as a function of Q^2 from JLab, as well as previous data SLAC.

measure the difference of $R_A - R_P$.

The $R_A - R_D$ difference can be extracted with Rosenbluth technique, i.e. linear fitting the A/P cross section ratios at different ϵ settings. For small R and two ϵ points, $R_A - R_D$ only depends on a double cross section ratio:

$$R_A - R_D \approx \frac{1 - \frac{d\sigma_{1A}}{d\sigma_{1D}} \cdot \frac{d\sigma_{2D}}{d\sigma_{2A}}}{\epsilon_2 - \epsilon_1} \tag{10}$$

We proposal to compare F_L and R at the kinemtics shown in Table II and Figure 9. The projection for $R_A - R_D$ was shown in Figure 10 with a lot of systematic uncertainties canceled in the double cross section ratios.

In addition, we will study the Q^2 dependence of R. We expect $R \to 0$ at the real photon limit of $Q^2 \to 0$ at fixed ν. This trend was not observed in the Hall C measurement with 6 GeV beam at fixed x, as seen in Figure 11 [4]. However, if we study the Q^2 distribution at fixed ν instead of fixed x, we may see different Q^2 dependence. The fixed ν is equivalent to fixed W^2 at the limit of $Q^2 \to 0$.

We can extract R with Rosenbluth technique, i.e. linear fitting the differential cross sections at different ϵ settings. The relative difference between the differential cross sections are divided by the difference in ϵ to get the slope, i.e. R. Only the ratio of two differential cross sections is needed to extract R, where some systematic uncertainties are canceled. If we assume 1.8% in the cross section, then $\Delta R/R$ is about 20% at lower x. For the kinematics that can be accessed with three beam energies, the ϵ coverage is bigger and the uncertaity

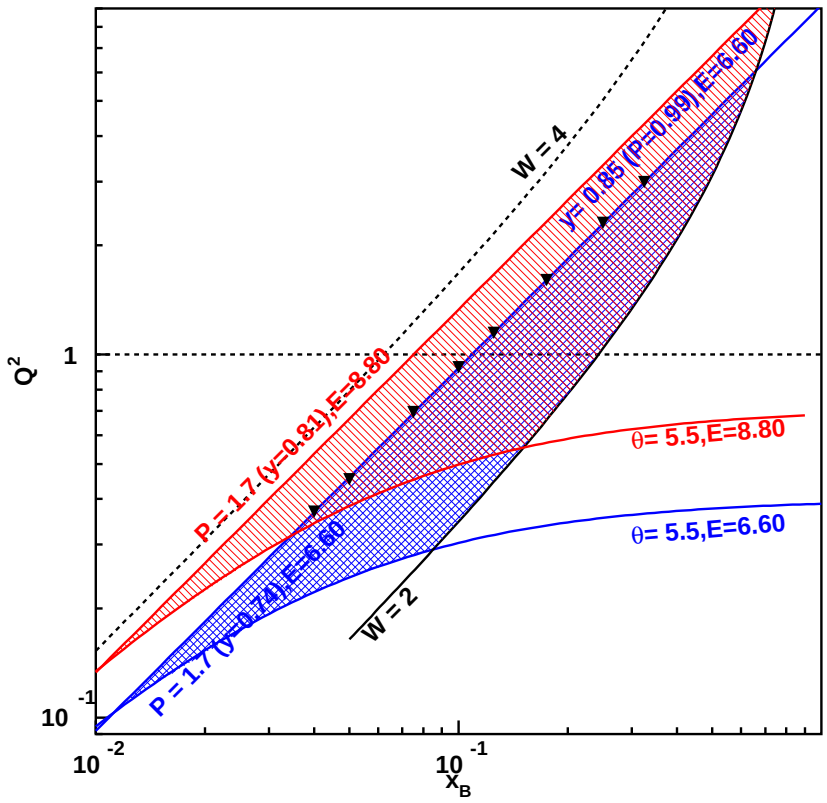

FIG. 9: The proposed kinematics to study the Q^2 dependence of R with SHMS/HMS spectrometer. The Rosenbluth separation can be done with 6.6, 8.8 GeV, and sometimes 11.0 GeV beam.

in R will be reduced. Assuming $R = 0.3$, the projected data are plotted in Figure 12.

One can also extract the longitudinal structure function F_L with the Rosenbluth technique from R, i.e. $F_L = R \cdot 2xF_1$. The F_L, identically zero in lowest order QCD, gets a non-zero value in perturbative QCD from gluon radiation. Measurements of F_L can thus provide constraints on the gluon density in the proton which are complementary to that obtained from the scaling violations of the F_2 structure function. Since R is generally small (~ 0.3), the uncertainty in F_L is dominated by that from the R.

Q^2	x_b	E	E'	θ	ϵ	y	W
0.369	0.040	6.6	1.7	10.4	0.477	0.742	3.12
0.364	0.040	8.8	3.9	5.9	0.737	0.557	3.12
0.453	0.050	6.6	1.7	11.6	0.476	0.742	3.10
0.455	0.050	8.8	3.9	6.6	0.737	0.557	3.10
0.695	0.075	6.6	1.7	14.3	0.472	0.742	3.06
0.685	0.075	8.8	3.9	8.1	0.734	0.557	3.06
0.687	0.075	11.	6.1	5.8	0.844	0.446	3.06
0.924	0.100	6.6	1.7	16.5	0.469	0.742	3.03
0.922	0.100	8.8	3.9	9.4	0.732	0.557	3.03
0.917	0.100	11.	6.1	6.7	0.843	0.446	3.03
1.147	0.125	6.6	1.7	18.4	0.465	0.742	2.99
1.149	0.125	8.8	3.9	10.5	0.730	0.557	2.99
1.148	0.125	11.	6.1	7.5	0.842	0.446	2.99
1.605	0.175	6.6	1.7	21.8	0.458	0.742	2.91
1.601	0.174	8.8	3.9	12.4	0.726	0.557	2.91
1.616	0.176	11.	6.1	8.9	0.848	0.446	2.91
2.306	0.250	6.6	1.7	26.2	0.447	0.742	2.79
2.308	0.251	8.8	3.9	14.9	0.719	0.557	2.79
2.290	0.249	11.	6.1	10.6	0.835	0.446	2.79
2.987	0.325	6.6	1.7	29.9	0.437	0.742	2.66
2.999	0.326	8.8	3.9	20.1	0.713	0.557	2.66
2.982	0.324	11.	6.1	12.1	0.831	0.446	2.66

TABLE II: The proposed kinematics to measure F_L and R with SHMS(red or black)/HMS (blue or black).

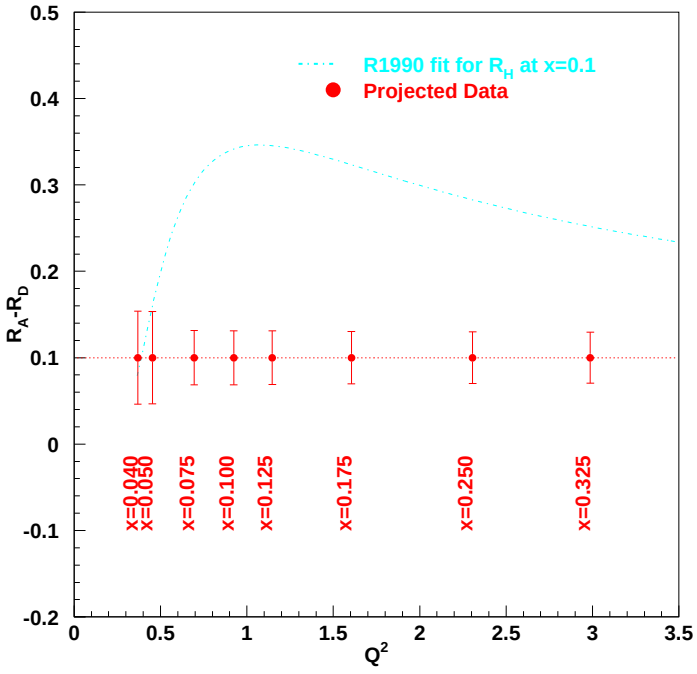

FIG. 10: The projected data for Q^2 dependence of $R_A - R_D$ at low Q^2. The uncertainties are estimated based on 1% relative uncertainty in cross sections ratios.

3.3. F_L moments at $Q^2 = 3.75$

In the NLO order, the F_L moments can be directly related to the gluon moments via the "gluon" sum rule [17]:

$$F_L^{[n]}(Q^2) = \frac{\alpha_s(Q^2)}{\pi}\left[\frac{4}{3(n+1)}F_2^{[n]}(Q^2) + \frac{2c}{(n+1)(n+2)}(xG)^{[n]}(Q^2)\right] \tag{11}$$

where $c = \sum_f e_f^2 = 2/3, 10/9, 11/9$ for number of quark flavors $N_f = 3, 4, 5$ respectively. The nth moment of the structure function $F(x, Q^2)$ is an integral over x, i.e. $F^{[n]}(Q^2) = \int_0^1 dx x^{n-2} F(x, Q^2)$. With inverse Mellin transform, the above equation can be changed into:

$$F_L(x, Q^2) = \frac{\alpha_s(Q^2)}{\pi}\left[\frac{4}{3}\int_x^1 \frac{dy}{y}(\frac{x}{y})^2 F_2(y, Q^2) + 2c\int_x^1 \frac{dy}{y}(\frac{x}{y})^2(1-\frac{x}{y})yG(y, Q^2)\right] \tag{12}$$

This equation was embedded in CTEQ PDFs.

Particularly for $n = 2$ and and $N_f = 3$, Equation 11 becomes:

$$\int_0^1 dx\ F_L(x, Q^2) = \frac{\alpha_s(Q^2)}{9\pi}\ \left[\ 4\ \int_0^1 dx\ F_2(x, Q^2) + \int_0^1 dx\ x\ G(x, Q^2)\ \right]. \tag{13}$$

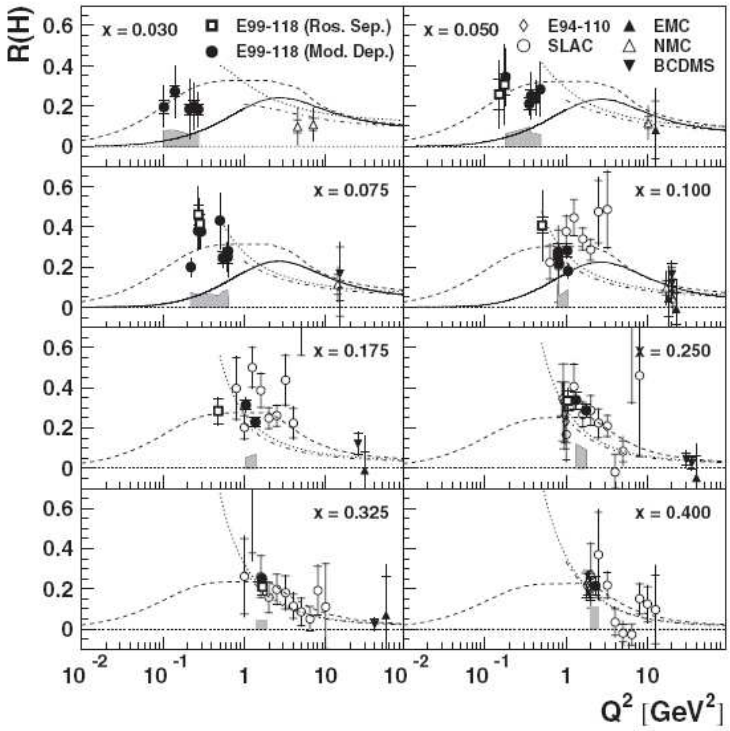

FIG. 11: [4] $R(x, Q^2)$ for hydrogen from JLab E99-118 experiment and other world measurements. The model dependent extraction of R is not as reliable as that with Rosenbluth technique. The dashed curves represent the JLab E99-118 parametrization, which assumes the form of $R_P = A(x)(1-e^{-bQ^2})$ for $Q^2 < 2$ and connects to SLAC Whitlow parametrization R_{1990} for $Q^2 > 2$. The fitted parameter $b = 9.212$ GeV^{-2}. The solid curves represent the model developed by Badelek, Kwiecinski and Staśto [23], based on the photon-gluon fusion mechanism. The dot-dashed curves are a next-to-next-to-leading order calculation based on MRST04 PDFs. The dotted curves show the next-to-leading order result of the GRV95 PDFs.

Measuring the F_L moments is one of the few direct probes of the gluonic structure of the nucleon. To measure the moments accurately, a range of x data must be obtained at fixed Q^2 to determine the integral shape and size. It also needs to cover the resonance region at large x and DIS region at small x. JLab E94-110 has some precision data on F_L in the resonance region from Q^2=0.75 to 3.75 [3]. In the DIS region, the existing data mainly came from SLAC, in a global re-analysis of existing data from different experiments, and the uncertainties can be improved in this dedicated experiment. In addition, we may combine the new data with the existing SLAC and JLab E94-110 data to expand ϵ coverage

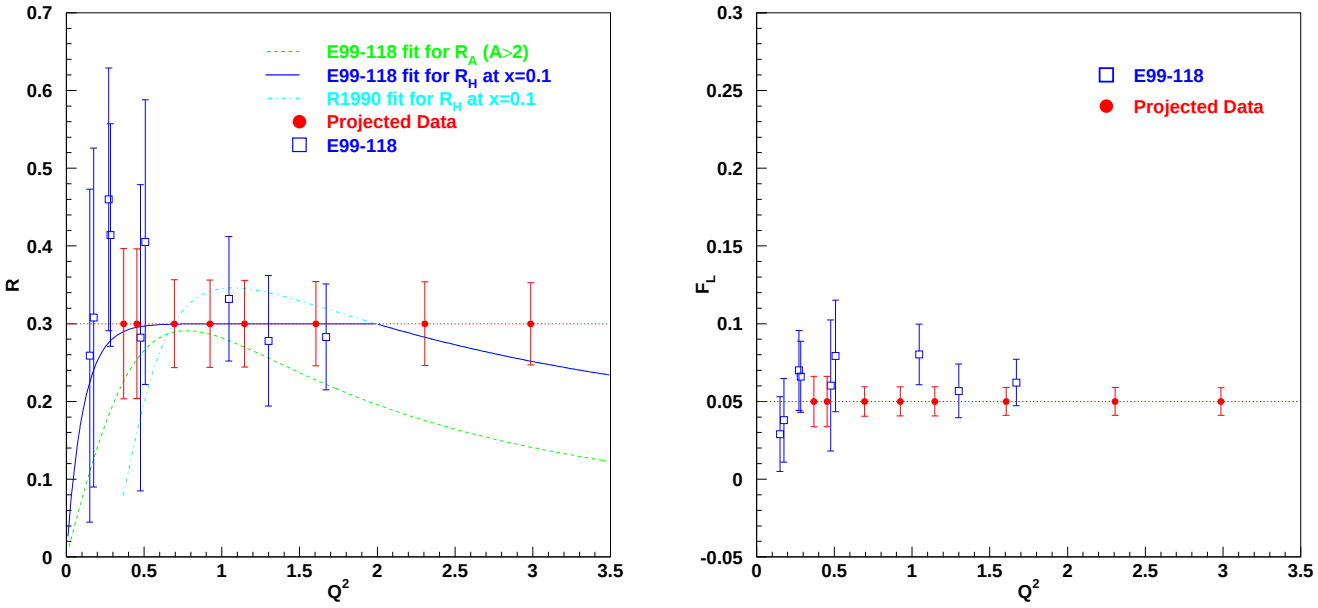

FIG. 12: The projected data for Q^2 dependence of R (left panel) and F_L (right panel) at low Q^2. The uncertainties are estimated based on 1.8% relative uncertainty in cross sections. The E99-118 data were estimated from the R and F_2 in Tvaskis's thesis.

and reduce their uncertainties. The low x region ($x < 0.25$) can not be reached directly at $Q^2 \sim 4.0$. It can be constrained indirectly by using existing SLAC data and taking new data at lower Q^2 at 0.75, 1.75 and 2.75 $(\mathrm{GeV/c})^2$, as shown in Figure 13 and Table III. The projected data will reduce the existing uncertainty for the $n = 4$ F_L moment by a factor of two [16].

We may also extract the difference between proton and neutron F_2 moments, and compare it with nucleon non-singlet QCD moments from the Lattice calculations at $Q2 = 4$ [18].

4. EXPERIMENT

4.1. Experimental Overview

The experiment will use the standard HMS and SHMS spectrometers for inclusive measurements of scattered electrons from the A(e, e')X reaction. Measurements will be performed on hydrogen, deuterium, the Al "dummy", and solid targets including C, Ca and

Q^2	x_b	E	E'	θ	ϵ	y	W
3.75	0.275	8.8	1.53	30.6	0.307	0.826	3.28
3.76	0.275	11.0	3.73	17.4	0.586	0.661	3.28
3.74	0.324	8.8	2.65	23.1	0.519	0.699	2.95
3.73	0.323	11.0	4.85	15.2	0.716	0.559	2.95
3.75	0.375	6.6	1.27	39.1	0.316	0.808	2.67
3.76	0.376	8.8	3.47	20.2	0.648	0.606	2.67
3.76	0.376	11.0	5.67	14.1	0.793	0.485	2.67
3.75*	0.425	5.5	0.80	55.0	0.211	0.855	2.44
3.74	0.424	6.6	1.90	31.7	0.473	0.712	2.44
3.77	0.427	11.0	6.30	13.4	0.841	0.427	2.44
3.75*	0.474	5.5	1.29	42.5	0.365	0.765	2.24
3.75	0.474	6.6	2.39	28.2	0.580	0.638	2.24
3.77	0.477	11.0	6.79	12.9	0.873	0.383	2.24
3.74*	0.524	5.5	1.69	37.0	0.478	0.693	2.07
3.76	0.525	6.6	2.79	26.1	0.657	0.577	2.07
3.75	0.524	11.0	7.19	12.5	0.895	0.346	2.07
3.75*	0.574	4.4	0.92	57.5	0.282	0.791	1.91
3.76*	0.575	5.5	2.02	33.8	0.562	0.633	1.91
3.74	0.572	6.6	3.12	24.6	0.713	0.527	1.92
3.74	0.572	11.0	7.52	12.2	0.912	0.316	1.92
3.76*	0.626	4.4	1.20	49.9	0.383	0.727	1.77
3.75*	0.625	5.5	2.30	31.6	0.626	0.582	1.77
3.75	0.625	6.6	3.40	23.6	0.754	0.485	1.77
3.75	0.624	11.0	7.80	12.0	0.924	0.291	1.77
3.75*	0.674	4.4	1.44	45.2	0.463	0.673	1.64
3.74*	0.674	5.5	2.54	30.0	0.676	0.538	1.64
3.75	0.676	6.6	3.64	22.8	0.787	0.448	1.64
3.74	0.673	11.0	8.04	11.8	0.933	0.269	1.64
3.75*	0.725	4.4	1.64	42.3	0.525	0.791	1.52
3.75*	0.725	5.5	2.74	28.9	0.713	0.502	1.52
3.76	0.725	6.6	3.82	22.2	0.811	0.418	1.52
3.77	0.727	11.0	8.24	11.7	0.940	0.251	1.51

TABLE III: The kinematics to measure the F_L moments at $Q^2 = 3.75$ GeV^2 with SHMS(red or black)/HMS (blue or black). The kinematics with stars(*) (green) are existing data.

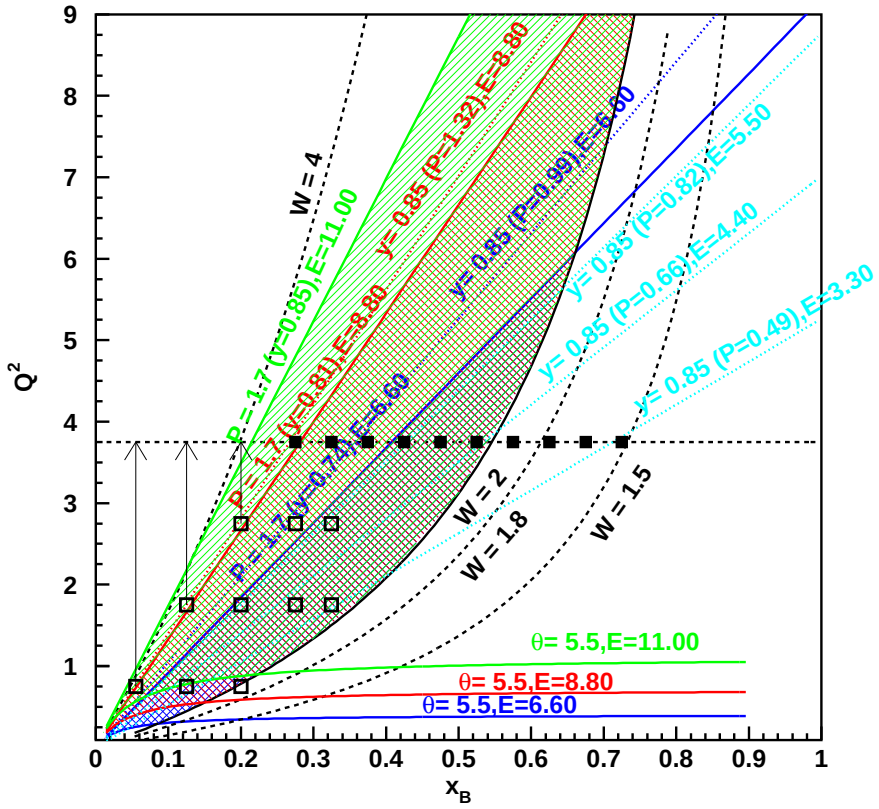

FIG. 13: The proposed kinematics to F_L moments measurement at $Q^2 = 3.75$ GeV^2. The low x points may be evolved from lower Q^2.

Sn. The production rates are very high for our kinematics, therefore 10cm cryogenic target (better with 4cm) and thin solid targets (1% radiation length) will be used. Calcium can be easily oxidized in the air, so we will keep it in an oil substance before transposing it to the scattering chamber vacuum. A "glove box" is necessary for the handling of the Calcium target. This will be available before the 11 GeV experiments since 4% RL ^{40}Ca and ^{48}Ca targets will be used in the approved short range correlation experiment E08-014 [25].

4.2. Systematic Uncertainty

The systematic uncertainty is the dominant one at low Q^2 and low x region. Generally speaking, the systematic uncertainty with 12 GeV upgrade will be similar to what we had before. Referring to JLab E99110 [26] and E99-118 experiment [4], the systematic uncer-

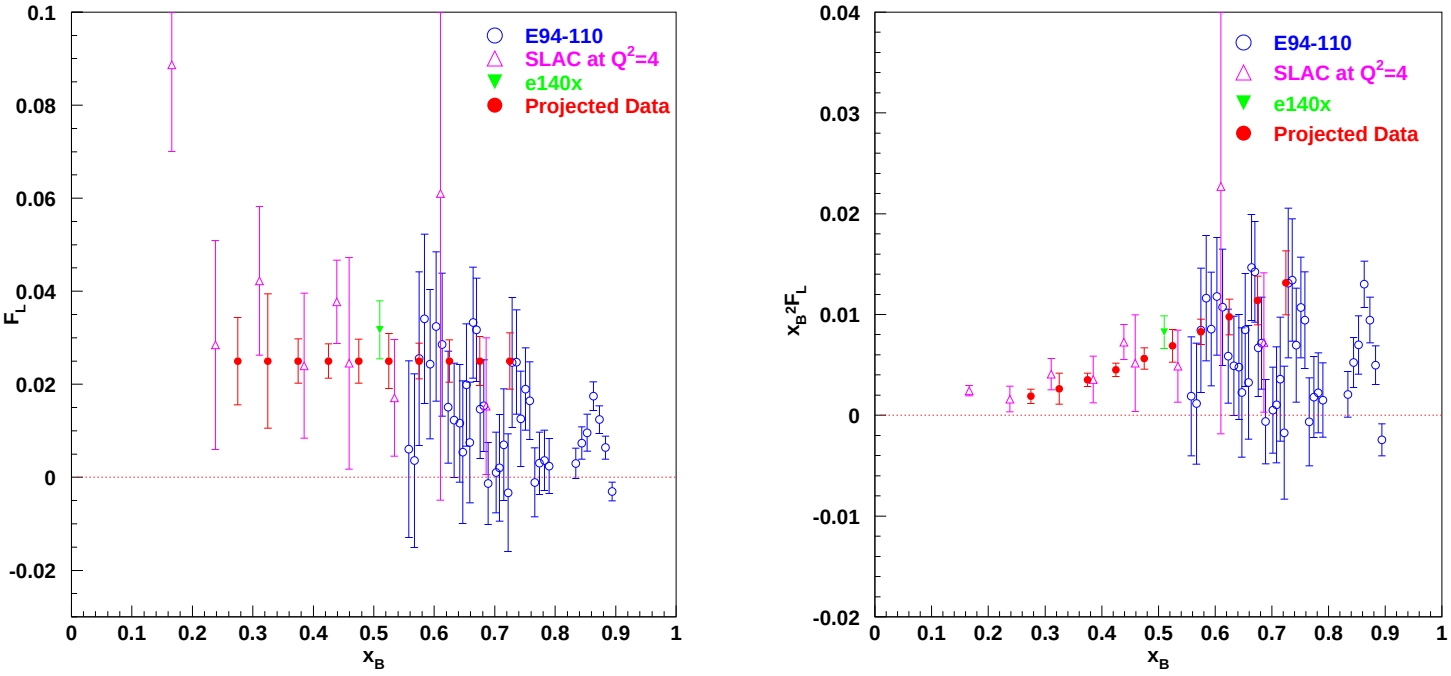

FIG. 14: The projected F_L and x^2F_L as a function of Bjorken x_B at $Q^2 = 3.75$ GeV^2, as well as the existing world data. The uncertainties are estimated assuming 1.5% relative uncertainty in cross sections ratios with the Whitlow's parameterization for R values(R_{1990}). For the $x > 0.5$ points, the new measurement will add two high ϵ points to the existing E94-110 resonance data and reduce the current uncertainties significantly. There is also potential to reduce the uncertainty of the data in the DIS region by combining the proposed data and the SLAC data.

tainties are estimated in Table IV. The total systematic uncertainty in the differential cross section is taken as the sum in quadrature of all systematic errors of the quantities that make up the cross section. The error propagation is based on the approximation at low Q^2:

$$\frac{d^2\sigma}{dE'd\Omega} \sim \sigma_T \sim \frac{1}{E^2(\theta^2)} \tag{14}$$

4.3. Beam Time Request

We would use standard beam energies of 6.6, 8.8 and 11 GeV. The energy change time was assumed to be 8 hours. However, extra non-standard beam energy like 7.7 GeV will help

Quantity	Uncertainty	$d\sigma_{DIS}/\sigma_{DIS}$ pt-pt
Beam Energy	0.04%	0.1%
Beam Charge	0.2 μ A	0.5 (*40/I)%
Scattered Electron Energy	0.04%	<0.1 %
Electronic Dead Time	0.25%	0.25%
Computer Dead Time	0.2%	0.2%
Tracking Efficiency	0.3%	0.3%
Detector Efficiency	0.2%	0.2%
Charge Symmetric Background	0.4%	0.4%
Acceptance	0.6%	0.6%
Scattered Electron Angle	0.5 mr	1.0 (*5.5/θ) %
Cryogenic Target Density	0.1%	0.1%
Cryogenic Target length	0.1%	0.1%
Cryogenic Target Background	0.3%	0.3%
Radiative Correction	1%	1% [a]
Total in Cryogenic Rosenbluth Separation	1.8%(1.5% at $\theta > 11.0$)	
Total in Nuclear Rosenbluth Separation	1.7%	
Total in Nuclear/Cryogenic Ratio	1.1%	

[a]It can be bigger for some kinematics.

TABLE IV: Point-to-Point systematic uncertainties in the DIS cross section due to the uncertainty in various experimental quantities.

to reduce the uncertainties. In addition, the existing data at lower energies will be combined to increase ϵ span and reduce uncertainties. Rates for these experiments will be generally high, the uncertainties are dominated by the systematic uncertainties. It is crucial to take a complete set of optics calibration data especially on SHMS. The optics data need to be taken for HMS for cross-calibration. The momentum scan and angle scan with overlapping acceptance but different central setting is very important for the future analysis with finer binning. It will benefit future experiments in Hall C too.

Only one spectrometer is required for each kinematics. The other spectrometer can be

used to monitor the positron background and the luminosity to control systematic uncertainties. We will try to use a single beam current of 40 μA for all kinematics. We may have to reduce the beam current for Calcium target and for the kinematics with the high rates. A beam current calibration is proposed for this experiment.

The beam time request is summarized in Table V. We will have quite many kinematics which also requires many kinematics/target changes. Assuming an average beam time of 30 minutes for each setting and an average overhead of 6 minutes for each angle/target change and 18 minutes for each momentum change, the total requested beam time is 263.1 hours (11 days).

Item		Beam Time (Hours)
Production	F_2 Measurements on D, C, Al, Ca, Sn	25*5*0.5= 62.5
	R Measurements on H, D, Al, C, Ca, Sn	22*6*0.5= 66.0
	F_L Moments on H, D and Al	41*3*0.5= 61.5
Calibration	Optics (Sieve/Open Collimator; P/θ scan)	24.
	Beam Current Calibration	8.
	Target Boiling Studies	8.
Others	Beam Energy Changes	2*8=16
	Target Changes	292*0.1=29.2
	Angle Changes	35*0.1=3.5
	Momentum Changes	50*0.3=15.0
Total		263.1 (11 days)

TABLE V: Beam time request assuming 100% efficiency. An average beam time of 30 minutes were assumed for each production kinematics and additional 12 minutes for each kinematic/target change.

5. SUMMARY

We propose to do three related sets of inclusive cross section measurements, with the standard equipment in Hall C after the 12 GeV upgrade, on various nuclei (H,D,Al,C,Ca,Sn) in the range $0.2 < Q^2 < 3.8$ (GeV/c)^2. First, we propose to measure the Q^2 dependence in

the nuclear ratios of F_2 at $0.01 < x < 0.1$ and check the Sn/C F_2 data from the NMC, which plays an unique role in affecting the global fit of the nuclear PDFs. Second, we propose to study the nuclear dependence of F_L and R in the range of $0.4 < Q^2 < 3.3$ (GeV/c)^2, since the existing data suggest nonzero $R_D - R_P$ at low Q^2. Finally we will measure and improve F_L at $Q^2 = 3.75$ (GeV/c)^2 with hydrogen and deuterium targets over a range of x. This will significantly reduce the uncertainty in higher F_L moments, which is directly related to gluon moments in pQCD.

6. COMMITMENT TOWARD THE BASE EQUIPMENT CONSTRUCTION

The collaboration has a strong commitment to support the equipment for Hall C at 12 GeV. In particular, we note that Hampton University is responsible for leading the construction of the drift chambers for the SHMS spectrometer. The design of the drift chambers is nearly completed and construction will begin soon under the direction of one of the spokespersons. Progress is reported regularly to the SHMS collaboration, which will next meet just prior to PAC35. Further commitments include the installation of the chambers into the detector hut and commissioning.

---

[1] I. Schienbein *et al.*, Phys. Rev. D **80**, 094004 (2009);I. Schienbein *et al.*,Phys. Rev. D **77**, 054003 (2008); Tzvetalina Stavreva, Private Communication.

[2] M. N. Rosenbluth, Phys. Rev. **79**, 615 (1956).

[3] Y. Liang *et al.*, nuc-ex/0410027; E94-110 experiment, spokesperson: C.E. Keppel, *Measurement of $R = \sigma_L/\sigma_T$ in the Nucleon Resonance Region.*

[4] V. Tvaskis *et al.*, Phys. Rev. Lett. **98**, 142301 (2007) (nucl-ex/0611023); Vladas Tvaskis, Ph.D Thesis, *Longitudinal-Transverse Separation of Deep-Inelastic Scattering at low Q^2 on Nucleons and Nuclei*, Vrije Universiteit (2004); E99-118 experiment, spokespersons: A. Bruell, J. Dunne, and C.E. Keppel, *Measurement of the Nuclear Dependence of $R = \sigma_L/\sigma_T$ at Low Q2.*

[5] E00-002 experiment, spokespersons: C.S. Armstrong and M. I. Niculescu, *F2N at Low Q2.*

[6] E02-109 experiment, spokespersons: M. E. Christy and C.E. Keppel, *Measurement of $R =$*

σ_L/σ_T *on Deuterium in the Nucleon Resonance Region.*

[7] E04-001 experiment, spokespersons: A. Bodek and C.E. Keppel, *Measurements of F2 and R on Nuclear Targets in Resonance Region.*

[8] E06-009 experiment, spokespersons: M. E. Christy and C.E. Keppel, *Measurement of* $R = \sigma_L/\sigma_T$ *on Deuterium in the Nucleon Resonance Region and Beyond.*

[9] J. J. Aubert *et al.*, Phys. Lett. B **123**, 275 (1983).

[10] B. Reisert, A. S. Vera and Z. Zhang, *Structure Functions and Low-x Working Group Summary*, arXiv:0908.2194[hep-ex].

[11] L. W. Whitlow *et al.*, Phys. Lett. B **250**, 193 (1990); L. W. Whitlow, Ph.D. Thesis, SLAC-REPROT-357, Standford University (1990).

[12] L. H, Tao *et al.*[E140X Collaboration], Z. Phys. C **70**, 387 (1996).

[13] P. Amaudruz *et al.*[NMC Collaboration], Nucl. Phys. B **441**, 3 (1995).

[14] M. Arneodo *et al.*[NMC Collaboration], Nucl. Phys. B **441**, 12 (1995).

[15] M. Arneodo *et al.*[NMC Collaboration], Nucl. Phys. B **481**, 23 (1996).

[16] Peter Monaghan, Private Communication.

[17] R. G. Roberts, *The structure of the proton: Deep Inelastic Scattering*, Cambridge University Press, p88,p95 (1990).

[18] D. Dolgov *et al*, Phys. Rev. D **66**, 034506 (2002); M. Göckeler *et al* [QCDSF Collaboration], Phys. Rev. D **71**, 114511 (2005); W. Detmold , W. Melnitchouk and A. W. Thomas, Phys. Rev. D **66**, 054501 (2002).

[19] I. Niculescu, J. Arrington, R. Ent and C. E. Keppel, Phys. Rev. C **73**, 045206 (2006).

[20] M. Hirai, S. Kumano and T.-H. Nagai,Phys. Rev. C **76**, 065207 (2007).

[21] K. Ackerstaff *et al.*[HERMES Collaboration], Phys. Lett. B **475**, 386 (2000) and erratum, Phys. Lett. B **567**, 339 (2003);

[22] M. McDermott, L. Frankfurt, V. Guzey, and M. Strikman, Eur. Phys. J. C **16**, 641 (2000); Vadim Guzey, Private Communication.

[23] B. Badelek, J. Kwiecinski, and A. Staśto, Z. Phys. **C74**, 297 (1997).

[24] D.E. Wiser, Ph.D thesis, U. Wisconsin, 1977 (unpublished).

[25] JLab E08-014 experiment, spokespersons: J. Arrington, P. Solvignon, D. Higinbotham and D. B. Day, *Three-nucleon short range correlations studies in inclusive scattering for* $0.8 < Q^2 < 2.8$ *(GeV/c)*^{2} .

[26] M. E. Christy, Phys. Rev. C **70**, 015206 (2004).

[27] M. Hirai, S. Kumano, T.-H. Nagai, Phys. Rev. C **76**, 065207 (2007).